DALTON
FULL PAPER

Syntheses, structures, spectra and redox properties of alkoxo- and phenoxo-bridged diiron(III) complexes

Halikhedkar Aneetha,[a] Kaliyamoorthy Panneerselvam,[b] Tien-Fu Liao,[a] Tian-Huey Lu[b] and Chung-Sun Chung*[a]

[a] *Department of Chemistry, National Tsing Hua University, Hsinchu, 30043, Taiwan, Republic of China*
[b] *Department of Physics, National Tsing Hua University, Hsinchu, 30043, Taiwan, Republic of China*

Received 16th March 1999, Accepted 10th June 1999

Dinuclear di(μ-alkoxo) bridged $[Fe_2L^1_2]$ **1** (L^1 = trianion of 1,3-bis(salicylideneamino)propan-2-ol) and $[Fe_2L^2_2]$ **2** (L^2 = trianion of 1,3-bis(salicylamino)propan-2-ol) and di(μ-phenoxo) bridged $[Fe_2L^3_2]$ **3** (L^3 = trianion of 4-methyl-2,6-bis(salicylideneaminomethyl)phenol) and $[Fe_2L^4_2]$ **4** (L^4 = trianion of 4-methyl-2,6-bis(salicylaminomethyl)phenol) complexes have been synthesized and characterized. The crystal structure of **1** contains two molecules in the asymmetric unit and each molecule has two FeN_2O_4 distorted octahedral co-ordination units. The structure of **2** consists of a centrosymmetric dimer where the two crystallographically equivalent metal ions are asymmetrically bridged by two alkoxo oxygen atoms. The iron(III) centers have N_2O_4 co-ordination cores with amine nitrogens and phenolate oxygens in *cis* position. The crystal structure of **3** contains *trans*-FeN_2O_4 distorted octahedral co-ordination units bridged by two phenoxo oxygen atoms. The electronic spectra of all the complexes are characterized by high intensity charge-transfer transitions. Cyclic voltammetric studies of **1**, **3** and **4** in dichloromethane solvent reveal stepwise reduction of $Fe^{III}Fe^{III}$ to mixed-valence $Fe^{III}Fe^{II}$ and reduced $Fe^{II}Fe^{II}$ species while **2** exhibits a single quasireversible reduction peak corresponding to the mixed-valence form.

Introduction

Dinuclear metal complexes continue to attract attention largely due to their biological relevance.[1] The presence of oxo-bridged diiron centers in a variety of non-heme proteins[2–5] and enzymes has resulted in the synthesis and characterization of a large number of oxo and hydroxo (alkoxo or phenoxo) bridged diiron complexes in an effort to model such active sites.[6–10] The studies have shown that complexes display antiferromagnetic exchange coupling comparable to the biological systems. Considerable effort has been made to correlate the size and the extent of the magnetic exchange J parameter with the nature of the bridge and the geometries of the bridging atoms in the crystalline form.[11,12]

The complexes are also investigated for their interesting electronic and redox properties[10,12] and their use as catalysts for the oxidation of hydrocarbons.[13] During the course of our work on dinuclear complexes we have isolated a dialkoxo bridged diiron(III) complex with unique co-ordination mode of the ligands. Here we report the synthesis, structure, spectra and redox properties of this complex derived from the flexible 1,3-bis(salicylamino)propan-2-ol, H_3L^2, along with the structure and properties of dimeric complexes obtained from the analogous trianionic, pentadentate ligands H_3L^1, H_3L^3 and H_3L^4.

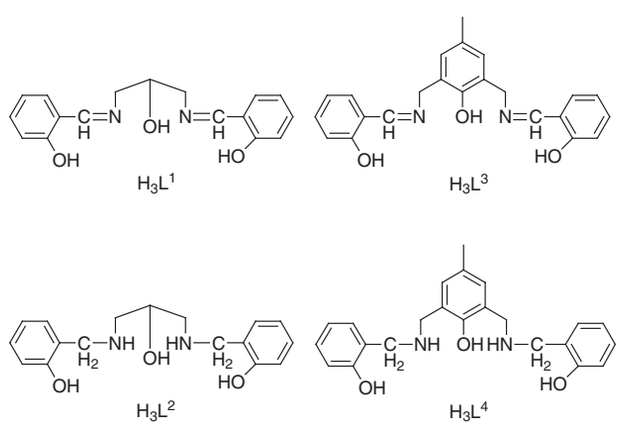

Experimental

Salicylaldehyde, 1,3-diaminopropan-2-ol and anhydrous iron(III) chloride were obtained from Merck and used as such. 2,6-Bis(aminomethyl)-4-methylphenol monohydrochloride,[14] the ligands H_3L^1, H_3L^3 and H_3L^4 were synthesized by the reported procedures.[15–17] All the solvents were purified by the standard procedures before use.[18]

Syntheses

H_3L^2. To a methanol solution (30 cm^3) of H_3L^1 (1.2 g, 4 mmol), was added sodium tetrahydroborate (0.31 g, 8 mmol) while stirring. The solution slowly became colorless. It was then diluted with 20 cm^3 of water. Methanol was removed on a rotary evaporator and the ligand extracted with dichloromethane solvent (2 × 30 cm^3). The dichloromethane layer was dried over anhydrous $MgSO_4$ and then evaporated to dryness to give a white crystalline residue. Yield 80%. ^1H NMR ($CDCl_3$): δ 2.71 (4 H, m, CH_2), 3.98 (1 H, m, CH), 4.04 (4 H, s, CH_2), 6.77 (4 H, m, aryl) 6.98 (2 H, m, aryl) and 7.18 (2 H, m, aryl). ^{13}C NMR ($CDCl_3$): δ 52.2, 68.7, 116.2, 119.1, 122.3, 128.5, 128.7 and 157.7.

$[Fe_2L^1_2]$ 1. To a stirred solution of H_3L^1 (0.596 g, 2 mmol) in 25 cm^3 of dry methanol were added anhydrous $FeCl_3$ (0.324 g, 2 mmol) and triethylamine (0.66 g, 6 mmol). In a few minutes an orange crystalline precipitate was obtained which was filtered off, washed with cold methanol and dried under vacuum. The complex was recrystallized from a mixture of dichloromethane and acetonitrile. Yield 75% (Found: C, 57.9;

Table 1 Electronic spectral and cyclic voltammetric data

Complex	UV/VIS[a] λ_{max}/nm (ε/dm^3 mol^{-1} cm^{-1})	Redox data[b] $E_{1/2}$/V (ΔE/mV)		Comproportionation constant,[c] K_{com}
		Fe^{III}–Fe^{II}	Fe^{II}–Fe^{II}	
$[Fe_2L^1_2]$	465 (3250), 327 (sh)	−0.75 (80)	−1.35 (200)	1.4×10^{10}
$[Fe_2L^2_2]$	440 (3650), 310 (sh)	−0.95 (260)	—	—
$[Fe_2L^3_2]$	472 (2210), 313 (sh)	−0.62 (70)	−1.14 (190)	6.3×10^{8}
$[Fe_2L^4_2]$	484 (2380), 306 (sh)	−0.62 (75)	−1.38 (195)	7.1×10^{12}

[a] In CH_2Cl_2. [b] In CH_2Cl_2 at 298 K (scan rate = 100 mV s^{-1}) using 0.1 mol dm^{-3} NBu_4ClO_4 as supporting electrolyte at a platinum working electrode with Ag–AgCl as reference electrode. [c] $\Delta E_{1/2} = (RT/F)\ln K$, $E_{1/2}(Fe^{III}Fe^{II}) - E_{1/2}(Fe^{II}Fe^{II})$ and K is the comproportionation constant.[10,12,26,27]

H, 4.1; N, 7.8. $C_{34}H_{30}Fe_2N_4O_6$ requires C, 58.2; H, 4.3; N, 7.9%). IR/cm^{-1} (KBr) 1625 [ν(C=N)]. Magnetic moment (298 K) $\mu_{eff/Fe} = 5.18\ \mu_B$. Complex **1** was also obtained in reasonable yield even in the absence of the base.

$[Fe_2L^2_2]$ 2. To a stirred solution of H_3L^2 (0.604 g, 2 mmol) in 20 cm^3 of THF were added triethylamine (0.66 g, 6 mmol) and anhydrous $FeCl_3$ (0.324 g, 2 mmol) in 5 cm^3 of methanol. The reaction mixture was stirred for 30 min during which time complex **2** deposited as a bright red crystalline solid in quantitative yield. It was filtered off, washed with cold methanol and dried in vacuum. The complex was recrystallized from a dichloromethane and acetonitrile mixture. Yield 72% (Found: C, 57.2; H, 4.6; N, 7.7. $C_{34}H_{34}Fe_2N_4O_6$ requires C, 57.8; H, 4.9; N, 7.9%). IR/cm^{-1} (KBr) 3180 [ν(NH)] and 1605 [δ(NH)]. Magnetic moment (298 K) $\mu_{eff/Fe} = 5.10\ \mu_B$.

$[Fe_2L^3_2]$ 3. This complex was obtained in 70% yield in the same way as **1** using H_3L^3. It was recrystallized from dichloromethane (Found: C, 64.4; H, 4.3; N, 6.3. $C_{46}H_{38}Fe_2N_4O_6$ requires C, 64.7; H, 4.5; N, 6.6%). IR/cm^{-1} (KBr) 1620 [ν(C=N)]. Magnetic moment (298 K) $\mu_{eff/Fe} = 5.25\ \mu_B$.

$[Fe_2L^4_2]$ 4. To a stirred solution of H_3L^4 (0.38 g, 1 mmol) in 20 cm^3 of dry methanol were added triethylamine (0.33 g, 3 mmol) and $FeCl_3$ (0.162 g, 1 mmol). The reaction mixture was stirred for 3 h. The solvent was removed on a rotatory evaporator to leave a sticky brown residue. It was dissolved in 10 cm^3 of dichloromethane and precipitated by slow addition of hexane while stirring. Yield 65% (Found: C, 64.1; H, 4.8; N, 6.2. $C_{46}H_{42}Fe_2N_4O_6$ requires C, 64.4; H, 4.9; N, 6.5%). IR/cm^{-1} (KBr) 3250 [ν(NH)] and 1590 [δ(NH)]. Magnetic moment (298 K) $\mu_{eff/Fe} = 5.32\ \mu_B$.

Physical measurements

The carbon, hydrogen and nitrogen analyses were carried out on a Heraeus CHN elemental analyzer. Infrared spectra were recorded on a BOMEN (Hartmann & Braun MB series) FT-IR spectrophotometer as KBr pellets, electronic absorption spectra on a Hitachi U-3300 UV/VIS spectrophotometer and ^{1}H NMR spectra on an AC Bruker 300 MHz NMR spectrometer. Magnetic susceptibility measurements were carried out at room temperature using a CAHN magnetic balance set-up. Diamagnetic corrections were made using Pascals constants.[19] Cyclic voltammetric studies were carried out on a CH instruments model 604A computer controlled electrochemical analyzer. All the experiments were performed under a dry nitrogen atmosphere in dichloromethane solvent using 0.1 M NBu_4ClO_4 as the supporting electrolyte. A three-electrode assembly comprising a platinum working electrode, a platinum auxiliary electrode and Ag–AgCl reference electrode was used. The ferrocene–ferrocenium couple was used as the redox standard.

Crystallography

Single crystals of $[Fe_2L^1_2]\cdot CH_2Cl_2$, **1** and $[Fe_2L^3_2]\cdot CH_2Cl_2$ **3** were obtained by diffusion of hexane into their dichloromethane solutions while those of $[Fe_2L^2_2]\cdot H_2O$ **2** were obtained by slow evaporation of an acetonitrile and dichloromethane solution. Data collection was carried out at ambient temperature on either Enraf-Nonius CAD-4 or Siemens SMART CCD diffractometers using graphite monochromatized Mo-Kα radiation. The data were corrected for absorption.[20,21] The structures were solved by the heavy atom method using SHELXS 97[22] and refined using SHELXL 97.[23] The important crystallographic parameters are given in Table 2. The water molecule present in the asymmetric unit of **2** is hydrogen bonded to phenolate oxygens O(1) [O(1)···OW(1) 3.065(2) Å] and O(3) ($-x + 1$, $-y + 1$, $-z + 1$) [O(3)···OW(1) 2.834(2) Å].

CCDC reference number 186/1508.

Results and discussion

Syntheses

Reactions of anhydrous iron(III) chloride with Schiff base ligands H_3L^1 and H_3L^3 in methanol resulted in the formation of dinuclear complexes **1** and **3**. The dimeric complexes **2** and **4** were synthesized by the reactions of anhydrous $FeCl_3$ with ligands H_3L^2 and H_3L^4 in the presence of triethylamine in tetrahydrofuran–methanol and methanol solvent respectively. Attempts to synthesize carboxylate bridged complexes[10] by the reaction of ligands with $FeCl_3$ or $Fe(ClO_4)_3$ in 1:2 ratio in the presence of sodium acetate or benzoate were unsuccessful and only dimeric complexes were obtained.

IR and electronic spectra

The IR spectra of the complexes **1** and **3** showed characteristic C=N stretching in the range of 1620 to 1630 cm^{-1}. Complexes **2** and **4** exhibited a shoulder at *ca.* 1590–1600 cm^{-1} and a band around 3150–3250 cm^{-1} corresponding to δ(N–H) and ν(N–H) respectively. The electronic spectra of all the complexes in dichloromethane solvent showed high intensity transitions in the region of 440 to 480 nm. The ligand field transitions in the high spin octahedral complexes are spin forbidden, and the high intensity bands observed are assigned to a transition from the p_π orbital of the phenolate oxygen atom to the half filled d_{π^*} orbitals of the iron.[24,25] The high energy transitions at ≈310 and at ≈280 nm arise from the intraligand transitions. The electronic spectral data are given in Table 1.

Structure of $[Fe_2L^1_2]\cdot CH_2Cl_2$ 1

The asymmetric unit of complex **1** consists of two crystallographically independent molecules. The ORTEP[28] drawing of one of the independent molecules along with the numbering scheme is shown in Fig. 1. A comparison of bond distances and bond angles for both the molecules show small variations in these parameters. Both the molecules have two *trans*-FeN_2O_2 co-ordination cores bridged by two alkoxo oxygen atoms. The Fe_2O_2 portion of the bridge units is perfectly planar in both the molecules with a maximum deviation of ±0.02 Å from the least squares Fe_2O_2 plane. The two alkoxo bridges in molecule B are

asymmetric while in A the alkoxo bridge involving O(5) [d(Fe(1)–O(5)) = 2.060(5), d(Fe(2)–O(5)) = 1.995(5) Å, Δd = 0.065 Å] is significantly asymmetric but the other alkoxo bridge is relatively symmetric.

The average Fe–O (phenolate) and Fe–N (azomethine) bond lengths are 1.930(6) and 2.140(6) Å respectively, comparable to the bond lengths in other iron(III) Schiff base phenolate complexes.[29,30] The Fe–N bond lengths are slightly shorter at the Fe(2) center. The average Fe–O (alkoxo) bond lengths of 2.030(5) Å is significantly greater than the bond lengths in other alkoxo bridged complexes.[30,31]

The two Fe(1)–O(2)–Fe(1) and Fe(1)–O(5)–Fe(1) bond angles are almost identical and lead to a Fe···Fe distance of 3.25 Å, comparable to that in the dialkoxo bridged iron(III) complex, $[Fe_2(SALPA)_2(SALPAH)_2]$[26] (SALPAH = monoanion of *N*-(3-hydroxypropyl)salicylaldimine) but much longer than in $[Fe_2L(OH)Cl_2]$ and $[Fe_2L(OCH_3)Cl_2]$ (L = trianion of trisalicylidenetriethylenetetramine).[6] The average O–Fe–O bridge angle is 73.6(2)° which leads to severe distortions in the remaining bond angles in the co-ordination sphere from the ideal octahedral geometry. The *cis* O(1)–Fe(1)–O(6) and O(3)–Fe(2)–O(4) bond angles show large deviations and are in the range 99.7–114.4°. In general all the *cis* and *trans* angles deviate from 90 or 180°, especially the equatorial *trans* angles show large distortions and are in the range 139.5–156.2°. The average *trans* N–Fe–N bond angle is appreciably linear at Fe(2) [171.2°] while it deviates considerably from linearity at Fe(1) [156.5°]. Selected bond distances and bond angles are given in Table 3.

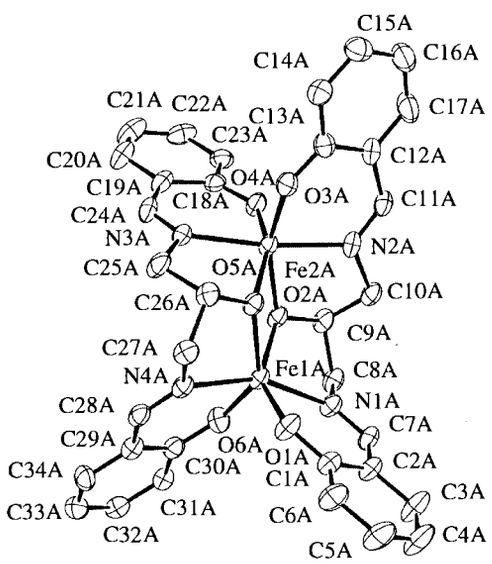

Fig. 1 An ORTEP drawing of the molecular structure of one of the two independent molecules forming the asymmetric unit of $[Fe_2L^1_2]$ **1**.

A consideration of metal planes reveals that the atoms O(1), O(2), O(5) and O(6) at Fe(1) and atoms O(2), O(3), O(4) and O(5) at Fe(2) in general deviate above or below the best planes of Fe(1) and Fe(2), however the deviation is more at Fe(1) [0.408–0.639 Å] than at Fe(2) [0.286–0.389 Å]. The dihedral angle between the planes of these two metal centers is 13.9(3)° in molecule A, 11.9(4)° in B.

Thus the crystal structure reveals that iron forms a di(μ-alkoxo) bridged complex rather than the proposed mono(μ-alkoxo) bridged structure with the second alkoxo oxygen atom in the terminal position.[32]

Structure of $[Fe_2L^2_2]\cdot H_2O$ 2

The complex has a centrosymmetric structure where the two crystallographically equivalent iron(III) centers are bridged by two alkoxo oxygen atoms. Unlike the Schiff base ligand H_3L^1, the highly flexible pentadentate ligand H_3L^2 winds itself around the five co-ordination sites of the metal ion in such a way that the two amine nitrogen atoms and two phenolate oxygen atoms are in the *cis* positions. The co-ordination sphere is completed by the alkoxo oxygen atom of the second ligand resulting in the formation of a unique dialkoxo bridged dimeric complex with two FeN_2O_4 co-ordination cores. The ORTEP drawing of the molecular structure along with the atom numbering scheme is given in Fig. 2. Selected bond lengths and angles are given in Table 4.

The dialkoxo bridge is highly asymmetric [d(Fe–O(2′)) = 1.990(1), d(Fe–O(2)) = 2.069(1) Å, Δd = 0.079 Å]. The presence of such an asymmetric Fe_2O_2 unit was recently established in $[Fe_2L_2(\mu\text{-}OCH_3)_2]$[33] ($\Delta d$ = 0.06 Å) (L = 1,2-bis(salicyl)ethane-1,2-diamine) and $[PH(t\text{-}Bu)_3]_2[Fe_2(\mu\text{-}OC_2H_5)_2Cl_6]$[34] ($\Delta d$ = 0.071 Å), while a symmetric bridge was observed in $[Fe_2(acac)_4(OC_2H_5)_2]$[35] and $[Fe_2(3,6\text{-}DBSQ)_4(\mu\text{-}OCH_3)_2]$[36] (DBSQ = 3,6-di-*tert*-butyl-1,2-benzosemiquinonate). Since the dimer lies on a crystallographic inversion center the bridging Fe_2O_2 ring is perfectly planar. The Fe–O–Fe bond angle of 100.8(1)° is much smaller than that in the other alkoxo bridged complexes while the O–Fe–O angle of 79.2(1)° is considerably widened compared to those in the other reported structures.[31,33] The Fe···Fe distance of 3.127(1) Å is comparable with those in $[Fe_2(acac)_4(OC_2H_5)_2]$[35] (3.116(1) Å) and $[Fe_2L(OMe)_2Cl_2]$[31] (3.144(1) Å) (L = dianion of 1,4-piperazinediylbis(N-ethylenesalicylaldimine) while it is much shorter than that in $[Fe_2(SALPA)_2(SALPAH)_2]$[29] (3.217(7)Å) and methoxophenoxo bridged diiron(III) complexes.[10] The Fe–O (phenolate) and Fe–N (amine) bond distances are in the expected range.[6,33,37,38]

Table 2 Crystallographic data for complexes $[Fe_2L^1_2]\cdot CH_2Cl_2$ **1**, $[Fe_2L^2_2]\cdot H_2O$ **2** and $[Fe_2L^3_2]\cdot CH_2Cl_2$ **3**

Formula	$C_{35}H_{32}Cl_2Fe_2N_4O_6$	$C_{34}H_{36}Fe_2N_4O_7$	$C_{47}H_{40}Cl_2Fe_2N_4O_6$
M	787.25	746.42	939.43
Crystal system	Triclinic	Triclinic	Triclinic
Space group	$P\bar{1}$	$P\bar{1}$	$P\bar{1}$
a/Å	13.880(3)	9.649(1)	10.0188(1)
b/Å	15.151(2)	9.723(1)	13.3004(2)
c/Å	19.557(2)	9.845(1)	15.9861(2)
α/°	94.36(1)	89.16(1)	84.622(1)
β/°	108.59(1)	80.78(1)	82.602(1)
γ/°	113.87(1)	66.10(1)	80.938(1)
V/Å^3	3463.5(9)	832.3(2)	2080.24(5)
Z	4	1	2
μ(Mo-Kα)/cm^{-1}	10.43	9.29	8.82
T/K	293	293	293
Reflections measured	15899	3824	19867
Reflections observed	8321 ($F > 4\sigma F$)	3356 ($F > 4\sigma F$)	4796 ($F > 6\sigma F$)
R(int)	0.0704	0.0116	0.0574
$R(F)$	8.7	2.8	5.5
$R'(F^2)$	25.9	7.4	12.9

Table 3 Selected bond lengths (Å) and angles (°) in $[Fe_2L^1_2]\cdot CH_2Cl_2$ **1**

Fe(1A)–O(6A)	1.916(6)	Fe(1A)–O(1A)	1.930(6)
Fe(1A)–O(2A)	2.040(5)	Fe(1A)–O(5A)	2.060(5)
Fe(1A)–N(4A)	2.163(7)	Fe(1A)–N(1A)	2.166(6)
Fe(2A)–O(4A)	1.928(6)	Fe(2A)–O(3A)	1.948(6)
Fe(2A)–O(5A)	1.995(5)	Fe(2A)–O(2A)	2.027(5)
Fe(2A)–N(2A)	2.109(6)	Fe(2A)–N(3A)	2.123(6)
Fe(1B)–O(1B)	1.915(6)	Fe(1B)–O(6B)	1.928(7)
Fe(1B)–O(5B)	2.047(6)	Fe(1B)–O(2B)	2.053(5)
Fe(1B)–N(1B)	2.147(7)	Fe(1B)–N(4B)	2.165(7)
Fe(2B)–O(4B)	1.928(5)	Fe(2B)–O(3B)	1.949(7)
Fe(2B)–O(5B)	2.006(5)	Fe(2B)–O(2B)	2.010(6)
Fe(2B)–N(3B)	2.112(7)	Fe(2B)–N(2B)	2.132(7)
Fe(1A)···Fe(2A)	3.250(2)	Fe(1B)···Fe(2B)	3.247(2)
O(6A)–Fe(1A)–O(1A)	110.2(3)	O(6A)–Fe(1A)–O(2A)	94.9(2)
O(1A)–Fe(1A)–O(2A)	145.6(3)	O(6A)–Fe(1A)–O(5A)	139.5(2)
O(1A)–Fe(1A)–O(5A)	99.6(2)	O(2A)–Fe(1A)–O(5A)	72.8(2)
O(6A)–Fe(1A)–N(4A)	83.0(3)	O(1A)–Fe(1A)–N(4A)	81.4(3)
O(2A)–Fe(1A)–N(4A)	126.1(2)	O(5A)–Fe(1A)–N(4A)	74.9(2)
O(6A)–Fe(1A)–N(1A)	86.3(3)	O(1A)–Fe(1A)–N(1A)	83.1(3)
O(2A)–Fe(1A)–N(1A)	75.2(2)	O(5A)–Fe(1A)–N(1A)	124.9(2)
N(4A)–Fe(1A)–N(1A)	156.8(3)	O(4A)–Fe(2A)–O(3A)	99.7(3)
O(4A)–Fe(2A)–O(5A)	156.8(2)	O(3A)–Fe(2A)–O(5A)	97.3(2)
O(4A)–Fe(2A)–O(2A)	95.1(2)	O(3A)–Fe(2A)–O(2A)	157.0(2)
O(5A)–Fe(2A)–O(2A)	74.4(2)	O(4A)–Fe(2A)–N(2A)	87.9(3)
O(3A)–Fe(2A)–N(2A)	85.0(3)	O(5A)–Fe(2A)–N(2A)	109.4(2)
O(2A)–Fe(2A)–N(2A)	77.9(3)	O(4A)–Fe(2A)–N(3A)	85.8(3)
O(3A)–Fe(2A)–N(3A)	91.5(2)	O(5A)–Fe(2A)–N(3A)	78.0(2)
O(2A)–Fe(2A)–N(3A)	107.2(2)	N(2A)–Fe(2A)–N(3A)	172.2(3)
Fe(2A)–O(5A)–Fe(1A)	106.1(2)	Fe(2A)–O(2A)–Fe(1A)	106.6(2)
O(1B)–Fe(1B)–O(6B)	114.4(3)	O(1B)–Fe(1B)–O(5B)	94.4(3)
O(6B)–Fe(1B)–O(5B)	141.6(3)	O(1B)–Fe(1B)–O(2B)	142.5(3)
O(6B)–Fe(1B)–O(2B)	95.2(3)	O(5B)–Fe(1B)–O(2B)	72.8(2)
O(1B)–Fe(1B)–N(1B)	83.6(3)	O(6B)–Fe(1B)–N(1B)	84.4(3)
O(5B)–Fe(1B)–N(1B)	125.4(3)	O(2B)–Fe(1B)–N(1B)	76.6(2)
O(1B)–Fe(1B)–N(4B)	83.4(3)	O(6B)–Fe(1B)–N(4B)	83.0(3)
O(5B)–Fe(1B)–N(4B)	75.4(3)	O(2B)–Fe(1B)–N(4B)	124.6(2)
N(1B)–Fe(1B)–N(4B)	156.2(3)	O(4B)–Fe(2B)–O(3B)	101.7(3)
O(4B)–Fe(2B)–O(5B)	156.6(3)	O(3B)–Fe(2B)–O(5B)	95.1(3)
O(4B)–Fe(2B)–O(2B)	96.0(2)	O(3B)–Fe(2B)–O(2B)	153.8(3)
O(5B)–Fe(2B)–O(2B)	74.6(2)	O(4B)–Fe(2B)–N(3B)	85.4(2)
O(3B)–Fe(2B)–N(3B)	90.2(3)	O(5B)–Fe(2B)–N(3B)	78.3(2)
O(2B)–Fe(2B)–N(3B)	110.6(3)	O(4B)–Fe(2B)–N(2B)	88.2(3)
O(3B)–Fe(2B)–N(2B)	83.8(3)	O(5B)–Fe(2B)–N(2B)	109.8(3)
O(2B)–Fe(2B)–N(2B)	77.5(3)	N(3B)–Fe(2B)–N(2B)	170.2(3)
Fe(2B)–O(2B)–Fe(1B)	106.1(2)	Fe(2B)–O(5B)–Fe(1B)	106.5(2)

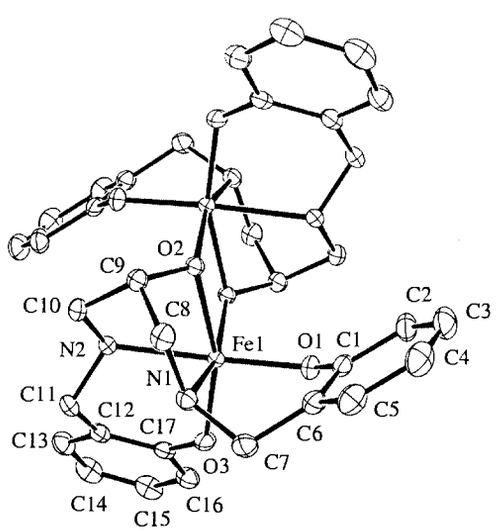

Fig. 2 An ORTEP drawing of the molecular structure of $[Fe_2L^2_2]$ **2** showing thermal ellipsoids at the 30% probability level along with the atom numbering scheme.

All the bond angles deviate from the ideal values, especially O(3)–Fe–O(2′) [102.63(5)°], O(2′)–Fe–N(1), [158.26(5)°] and O(3)–Fe–O(2) [161.76(5)°] show large deviations, making the co-ordination geometry distorted octahedral.

Table 4 Selected bond distances (Å) and angles (°) in $[Fe_2L^2_2]\cdot H_2O$ **2**

Fe(1)–O(3)	1.902(1)	Fe(1)–O(1)	1.916(1)
Fe(1)–O(2′)	1.990(1)	Fe(1)–O(2)	2.069(1)
Fe(1)–N(1)	2.186(2)	Fe(1)–N(2)	2.206(1)
Fe(1)···Fe(1′)	3.127(1)		
O(3)–Fe(1)–O(1)	98.93(6)	O(3)–Fe(1)–O(2′)	102.63(5)
O(1)–Fe(1)–O(2′)	98.63(5)	O(3)–Fe(1)–O(2)	161.76(5)
O(1)–Fe(1)–O(2)	98.71(5)	O(2)–Fe(1)–O(2′)	79.20(5)
O(3)–Fe(1)–N(1)	96.49(6)	O(1)–Fe(1)–N(1)	88.42(6)
O(2′)–Fe(1)–N(1)	158.26(5)	O(2)–Fe(1)–N(1)	79.41(5)
O(3)–Fe(1)–N(2)	87.71(5)	O(1)–Fe(1)–N(2)	169.54(5)
O(2′)–Fe(1)–N(2)	87.70(5)	O(2)–Fe(1)–N(2)	74.18(5)
N(1)–Fe(1)–N(2)	82.78(6)	C(1)–O(1)–Fe(1)	128.6(1)
C(9)–O(2)–Fe(1′)	133.0(1)	C(9)–O(2)–Fe(1)	105.48(9)
Fe(1)–O(2)–Fe(1′)	100.80(5)	C(17)–O(3)–Fe(1)	125.7(1)

Symmetry transformation used to generate equivalent atoms: $-x$, $-y+1$, $-z+1$.

Structure of $[Fe_2L^3_2]\cdot CH_2Cl_2$ 3

A perspective drawing of the molecular structure of complex **3** is given in Fig. 3. Selected bond lengths and angles are listed in Table 5. The asymmetric center consists of two iron(III) atoms bridged by two phenoxo oxygen atoms. The phenoxo bridge involving O(5) is asymmetric [*d*(Fe(1)–O(5) 1.999(3) Å) and *d*(Fe(2)–O(5) 2.046(4) Å, $\Delta d = 0.047$ Å], while the other phenoxo bridge is strongly asymmetric ($\Delta d = 0.075$ Å). Two phenolate oxygen atoms and two azomethine nitrogen atoms co-ordinate each metal ion in addition to the two bridging phenoxo oxygen atoms to give two *trans*-FeN_2O_4 co-ordination cores. One of the bridging phenolate rings is perpendicular and the angle between the two bridging rings is 85.7(2)°.

The average Fe–O (terminal) and Fe–N bond lengths are 1.915(4) and 2.154(4) Å respectively and are in the ranges normally observed for iron(III) Schiff base phenolate complexes[6,31] but the Fe–N distances are slightly longer than in the related $[Fe_2(SALAMP)_2]$ (SALAMP = 2-bis(salicylideneamino)methylphenolate) complex.[12] The average Fe–O (bridging) bond distance of 2.033(3) Å is shorter than in other phenoxo bridged complexes.[10,12]

All the *cis* and *trans* bond angles show large deviations from the ideal values, especially the equatorial transoid angles are kinked and are in the range 141.5–149.8°. The outer O(1)–Fe(1)–O(6) [113.4(2)°] and O(3)–Fe(2)–O(4) [114.6(2)°] bond angles are significantly widened and the *trans* N–Fe–N angle is linear at Fe(1) [170.9(2)°] while it deviates considerably from linearity at Fe(2) [157.7(2)°]. The two metal centers are held apart by 3.294(1) Å with two slightly different Fe–O–Fe angles of 109.1(2) and 107.5(2)°.

The severe distortion from the octahedral geometry in the complex appears to result from the bonding constraints of the ligand, and is also exhibited in the atom deviations from the best planes. The two iron and the two oxygen atoms of the four membered $Fe_2(\mu\text{-}O)_2$ ring are below and above respectively the least squares plane by ±0.123 Å and the oxygen atoms of the equatorial plane, O(1), O(2), O(5) and O(6) at Fe(1) and O(2), O(3), O(4), O(5) at Fe(2), also deviate from the least squares planes, rms deviation is ± 0.355 and ±0.447 Å respectively. The dihedral angle between the two planes is 50.91°.

Electrochemistry

Cyclic voltammetric studies of the complexes were carried out in dichloromethane solvent at a platinum electrode at scan rates of 50 to 200 mV s^{-1}. No significant differences were observed on changing the scan speed. Complex **1** exhibited a reversible wave at $E_{1/2} = -0.75$ V ($\Delta E = 80$ mV) followed by a quasi-reversible wave at −1.35 V ($\Delta E = 200$ mV) corresponding to the stepwise reduction of $Fe^{III}Fe^{III}$ to mixed-valence $Fe^{III}Fe^{II}$ and reduced $Fe^{II}Fe^{II}$ species respectively. Complex **3** also showed

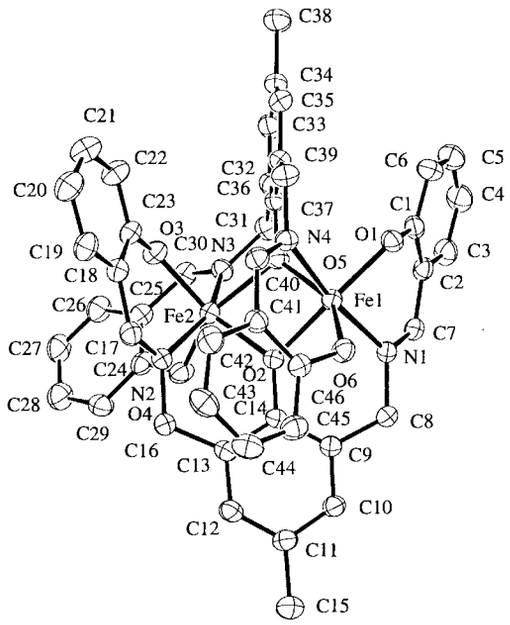

Fig. 3 An ORTEP drawing of the molecular structure of $[Fe_2L^3{}_2]$ **3**. Details as in Fig. 2.

Table 5 Selected bond lengths (Å) and angles (°) in $[Fe_2L^3{}_2]\cdot CH_2Cl_2$ **3**

Fe(1)–O(6)	1.912(4)	Fe(1)–O(1)	1.919(4)
Fe(1)–O(5)	1.999(3)	Fe(1)–O(2)	2.080(3)
Fe(1)–N(1)	2.115(4)	Fe(1)–N(4)	2.146(4)
Fe(2)–O(3)	1.916(4)	Fe(2)–O(4)	1.912(4)
Fe(2)–O(2)	2.005(3)	Fe(2)–O(5)	2.046(4)
Fe(2)–N(2)	2.167(4)	Fe(2)–N(3)	2.187(4)
Fe(1)···Fe(2)	3.294(1)		
O(6)–Fe(1)–O(1)	113.4(2)	O(6)–Fe(1)–O(5)	148.6(2)
O(1)–Fe(1)–O(5)	93.1(2)	O(6)–Fe(1)–O(2)	91.7(2)
O(1)–Fe(1)–O(2)	149.9(2)	O(5)–Fe(1)–O(2)	69.7(1)
O(6)–Fe(1)–N(1)	92.4(2)	O(1)–Fe(1)–N(1)	84.8(2)
O(5)–Fe(1)–N(1)	107.0(2)	O(2)–Fe(1)–N(1)	77.5(2)
O(6)–Fe(1)–N(4)	84.8(2)	O(1)–Fe(1)–N(4)	88.3(2)
O(5)–Fe(1)–N(4)	79.3(1)	O(2)–Fe(1)–N(4)	111.3(1)
N(1)–Fe(1)–N(4)	170.9(2)	O(3)–Fe(2)–O(4)	114.6(2)
O(3)–Fe(2)–O(2)	141.4(2)	O(4)–Fe(2)–O(2)	97.4(2)
O(3)–Fe(2)–O(5)	90.4(2)	O(4)–Fe(2)–O(5)	147.9(2)
O(2)–Fe(2)–O(5)	70.3(1)	O(3)–Fe(2)–N(2)	83.6(2)
O(4)–Fe(2)–N(2)	85.3(2)	O(2)–Fe(2)–N(2)	77.8(2)
O(5)–Fe(2)–N(2)	118.9(2)	O(3)–Fe(2)–N(3)	84.6(2)
O(4)–Fe(2)–N(3)	82.6(2)	O(2)–Fe(2)–N(3)	122.2(2)
O(5)–Fe(2)–N(3)	80.0(2)	N(2)–Fe(2)–N(3)	157.7(2)
Fe(1)–O(5)–Fe(2)	109.1(2)	Fe(1)–O(2)–Fe(2)	107.5(2)

stepwise reduction at −0.62 V and at −1.14 V. In this complex also the first electron transfer corresponding to mixed valence $Fe^{III}Fe^{II}$ species is reversible (ΔE = 70 mV) (Fig. 4). Comparison of the potentials of complexes **1** and **3** shows that in **1** the redox processes are significantly shifted to more cathodic potentials due to the greater electron density at the metal ions resulting from the alkoxo bridge. However, compared to $[Fe_2(SALAMP)_2]$, a diphenoxo bridged complex, the redox processes in **3** are significantly shifted to more negative potentials illustrating high electron density at each iron.[12]

Complex **2** shows a quasireversible wave (E_{pc} = −1.08 V, E_{pa} = −0.82 V) at 50 to 200 mV s^{-1} scan rates. This probably corresponds to the unstable mixed-valence $Fe^{III}Fe^{II}$ form. An irreversible redox process was reported for an analogous dimethoxo bridged dimeric complex at −1.13 V (*vs.* $Ag–Ag^+$) corresponding to a mixed-valence species, but no redox process for the second electron transfer was observed.[33] The triphenolate complex **4** shows a reversible first electron transfer process corresponding to the mixed-valence species at the same

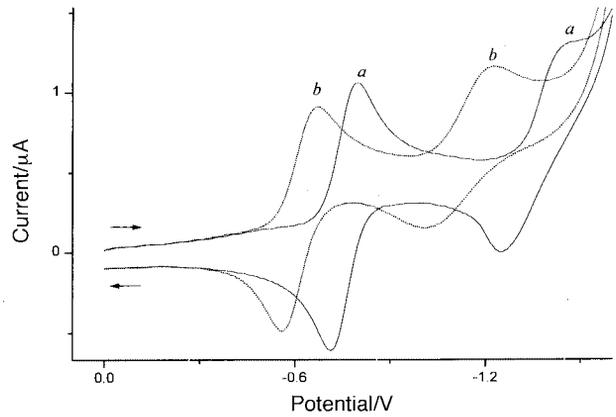

Fig. 4 Cyclic voltammograms at 298 K in CH_2Cl_2 solvent (0.1 mol dm^{-3} NBu_4ClO_4, Ag–AgCl reference electrode) at a platinum working electrode of complexes **1** (*a*) and **3** (*b*) at a scan rate of 100 mV s^{-1}.

potential (−0.62 V) as that of the iminophenolate **3**, however the potential corresponding to the formation of a reduced $Fe^{II}Fe^{II}$ species is shifted towards cathodic potential by 200 mV (−1.38 V) indicating enhanced stability of the mixed valence $Fe^{III}Fe^{II}$ species.

The stability of the $Fe^{III}Fe^{II}$ forms towards comproportionation evaluated by the corresponding constant *K* indicated that the mixed-valence forms are stabilized.[10,12,26,27] The redox data and the *K* values are given in Table 1.

Conclusion

Diiron(III) complexes from trianionic pentadentate ligands containing di(μ-alkoxo) or di(μ-phenoxo) bridges were synthesized and characterized. The crystal structures of di(μ-alkoxo) **1** and di(μ-phenoxo) **3** bridged complexes revealed severely distorted octahedral geometry at the metal center with two FeN_2O_4 co-ordination cores. Complex **4** is likely to have a more flexible co-ordination geometry due to the presence of the flexible CH_2NHCH_2 linkages. The flexible ligand H_3L^2 gave a dimeric complex containing two FeN_2O_4 co-ordination cores with the amine nitrogens and the phenolate oxygen atoms in *cis* position. Cyclic voltammetric studies of the complexes exhibited stepwise reduction of $Fe^{III}Fe^{III}$ to $Fe^{III}Fe^{II}$ and $Fe^{II}Fe^{II}$ species except for **2** where only a single quasireversible couple corresponding to the mixed-valence species was observed. Comproportionation constants calculated from the redox data indicated stable mixed-valence forms. Preliminary experiments have indicated that it is possible to isolate these species and a study of these complexes will be our future goal.

Acknowledgements

This research was supported by National Science Council (NSC), Taiwan (R. O. C.), Grant NSC-88-2113-M007-013 and NSC-88-2112-M-007-013. H. A. and K. P. thank NSC for postdoctoral fellowships.

References

1 L. Que, Jr. and R. C. Scarrow, in *Metal clusters in proteins*, ed. L. Que, Jr., American Chemical Society, Washington, D.C., 1988, p. 152.
2 R. G. Wilkins and P. C. Harrington, *Adv. Inorg. Biochem.*, 1983, **5**, 51; R. E. Stenkamp, L. C. Sieker, L. H. Jensen and J. Sanders-Loehr, *Nature* (*London*), 1981, **291**, 263; R. E. Stenkamp, L. C. Sieker and L. H. Jensen, *J. Am. Chem. Soc.*, 1984, **106**, 618; S. Sherrif, W. A. Hendrickson and J. L. Smith, *J. Mol. Biol.*, 1987, **197**, 273; B.-M. Sjoberg and A. Graslund, *Adv. Inorg. Biochem.*, 1983, **5**, 87; B. C. Antanaitis and P. Aisen, *Adv. Inorg. Biochem.*, 1983, **5**, 111.
3 L. Que, Jr. and A. E. True, *Prog. Inorg. Chem.*, 1990, **38**, 97.
4 J. Sanders-Loehr, in *Iron carriers and iron proteins*, ed. J. M. Loehr, VCH, New York, 1989, p. 373; A. L. Feig and S. J. Lippard, *Chem. Rev.*, 1994, **94**, 759.

5 S. J. Lippard, *Angew. Chem.*, *Int. Ed. Engl.*, 1988, **27**, 344; P. Nordlund, B.-M. Sjoberg and H. Eklund, *Nature* (*London*), 1990, **345**, 593.
6 B. Chiari, O. Piovesana, T. Tarantelli and P. F. Zanazzi, *Inorg. Chem.*, 1983, **22**, 2781; 1982, **21**, 2444; L. Borer, L. Thalken, C. Ceccarelli, M. Glick, J. H. Zang and W. M. Reiff, *Inorg. Chem.*, 1983, **22**, 1719.
7 K. Weighardt, K. Pohl and W. Gebert, *Angew. Chem.*, *Int. Ed. Engl.*, 1983, **22**, 727; J. R. Hartman, R. L. Rardin, P. Chaudhuri, K. Pohl, K. Weighardt, B. Nuber, J. Weiss, G. C. Papaefthymiou, R. B. Frankel and S. J. Lippard, *J. Am. Chem. Soc.*, 1987, **109**, 7387.
8 W. H. Armstrong and S. J. Lippard, *J. Am. Chem. Soc.*, 1984, **106**, 4632; W. H. Armstrong, A. Spool, G. C. Papaefthymiou, R. B. Frankel and S. J. Lippard, *J. Am. Chem. Soc.*, 1984, **106**, 3653.
9 B. P. Murch, P. D. Boyle and L. Que, Jr., *J. Am. Chem. Soc.*, 1985, **107**, 6728; S. Yan, L. Que, Jr., L. F. Taylor and O. P. Anderson, *J. Am. Chem. Soc.*, 1988, **110**, 5222; R. E. Norman, S. Yan, L. Que, Jr., G. Backes, J. Ling, J. Sanders-Loehr, J. H. Zhang and C. J. O'Connor, *J. Am. Chem. Soc.*, 1990, **112**, 1554; R. E. Norman, R. C. Holz, S. Menage, C. J. O'Connor, J. H. Zhang and L. Que, Jr., *Inorg. Chem.*, 1990, **29**, 4629.
10 S. Sandi-Urena and E. J. Parsons, *Inorg. Chem.*, 1994, **33**, 302; C. Belle, I. Gautier-Luneau, J.-L. Pierre, C. Scheer and E. Saint-Aman, *Inorg. Chem.*, 1996, **35**, 3706; K. Spartalian, J. A. Bonadies and C. J. Carrano, *Inorg. Chim. Acta*, 1988, **152**, 135.
11 D. M. Kurtz , Jr., *Chem. Rev.*, 1990, **90**, 585.
12 B. S. Snyder, G. S. Patterson, A. J. Abrahamson and R. H. Holm, *J. Am. Chem. Soc.*, 1989, **111**, 5214.
13 B. P. Murch, F. C. Bradley and L. Que, Jr., *J. Am. Chem. Soc.*, 1986, **108**, 5027; Y. Nishida, M. Takeuchi, H. Shimo and S. Kida, *Inorg. Chim. Acta*, 1984, **96**, 115; J. B. Vincent, J. C. Huffman, G. Christou, Q. Li, M. A. Nanny, D. N. Hendrickson, R. H. Fong and R. H. Fish, *J. Am. Chem. Soc.*, 1988, **110**, 6898.
14 M. Bell, A. J. Edwards, B. F. Hoskins, E. H. Kachab and R. Robson, *J. Am. Chem. Soc.*, 1989, **111**, 3603.
15 Y. Nishida and S. Kida, *J. Chem. Soc.*, *Dalton Trans.*, 1986, 2633.
16 W. Muzurek, A. M. Bond, K. S. Murray, M. J. O'Connor and A. G. Wedd, *Inorg. Chem.*, 1985, **24**, 2484.
17 S. K. Dutta, K. K. Nanda, U. Florke, M. Bhadbhade and K. Nag, *J. Chem. Soc.*, *Dalton Trans.*, 1996, 2371.
18 D. D. Perrin, W. L. F. Armarego and D. R. Perrin, *Purification of Laboratory Chemicals*, Pergamon, London, 1980.
19 E. A. Boudreaux and L. N. Mulay (Editors), in *Theory and applications of molecular paramagnetism*, Wiley, New York, 1976.
20 A. C. T. North, D. C. Phillips and F. S. Mathews, *Acta Crystallogr.*, *Sect. A*, 1968, **24**, 351.
21 G. M. Sheldrick, SHELXTL PLUS, Siemens Analytical X-Ray Instruments Inc., Madison, WI, 1990.
22 G. M. Sheldrick, *Acta Crystallogr.*, *Sect. A*, 1990, **46**, 467.
23 G. M. Sheldrick, SHELXL 97, *Program for refinement of crystal structures*, University of Göttingen, 1997.
24 B. P. Gaber, V. Miskowski and T. G. Spiro, *J. Am. Chem. Soc.*, 1974, **96**, 6868; E. W. Ainscough, A. M. Brodie, J. E. Plowman, K. L. Brown, A. W. Addison and A. R. Gainsford, *Inorg. Chem.*, 1980, **19**, 3655; M. G. Patch, K. P. Simolo and C. J. Carrano, *Inorg. Chem.*, 1983, **22**, 2630.
25 C. J. Carrano, K. Spartalian, G. V. N. Appa Rao, V. L. Pecoraro and M. Sundaralingam, *J. Am. Chem. Soc.*, 1985, **107**, 1651; C. J. Carrano, M. W. Carrano, K. Sharma, G. Backes and J. Sanders-Loehr, *Inorg. Chem.*, 1990, **29**, 1865; M. R. McDevitt, A. W. Addison, E. Sinn and L. K. Thompson, *Inorg. Chem.*, 1990, **29**, 3425.
26 R. R. Gagne, C. A. Koval, T. J. Smith and M. C. Cimolino, *J. Am. Chem. Soc.*, 1979, **101**, 4571.
27 S. K. Mandal, L. K. Thompson, K. Nag, J.-P. Charland and E. J. Gabe, *Inorg. Chem.*, 1987, **26**, 1391.
28 C. K. Johnson, ORTEP II, Report ORNL-5138, Oak Ridge National Laboratory, Oak Ridge, TN, 1976.
29 J. A. Bertrand and P. G. Eller, *Inorg. Chem.*, 1974, **13**, 927.
30 J. A. Bertrand, J. L. Breece and P. G. Eller, *Inorg. Chem.*, 1974, **13**, 125.
31 B. Chiari, O. Piovesana, T. Tarantelli and P. F. Zanazzi, *Inorg. Chem.*, 1982, **21**, 1396.
32 G. D. Fallon, A. Markiewicz, K. S. Murray and T. Quach, *J. Chem. Soc.*, *Chem. Commun.*, 1991, 198.
33 R. Vishwanathan, M. Palaniandavar, P. Prabhakaran and P. T. Muthiah, *Inorg. Chem.*, 1998, **37**, 3881.
34 D. Walker and R. Poli, *Inorg. Chem.*, 1990, **29**, 756.
35 B. Chiari, O. Piovesana, T. Tarantelli and P. F. Zanazzi, *Inorg. Chem.*, 1984, **23**, 3398.
36 A. S. Attia, B. J. Conklin, C. W. Lange and C. G. Pierpont, *Inorg. Chem.*, 1996, **35**, 1033.
37 M. Mikuriya, Y. Yamato and T. Tokii, *Chem. Lett.*, 1992, 1571.
38 K. K. Nanda, S. K. Dutta, S. Baitalik, K. Venkatsubramanian and K. Nag, *J. Chem. Soc.*, *Dalton Trans.*, 1995, 1239.

Paper 9/02068C